A motif of eleven amino acids is a structural adaptation that facilitates motor capability of eutherian prestin

Xiaodong Tan*, Jason L. Pecka, Jie Tang, Sándor Lovas, Kirk W. Beisel[‡,§] and David Z. Z. He[‡,§]

Department of Biomedical Sciences, Creighton University School of Medicine, 2500 California Plaza, Omaha, Nebraska, 68178, USA

*Present address: Department of Neuroscience, University of Wisconsin, Madison, WI 53706, USA
[‡]Shared last authorship
[§]Authors for correspondence (kirkbeisel@creighton.edu; hed@creighton.edu)

Accepted 26 September 2011
Journal of Cell Science 125, 1039–1047

doi: 10.1242/jcs.097337

Summary

Cochlear outer hair cells (OHCs) alter their length in response to transmembrane voltage changes. This so-called electromotility is the result of conformational changes of membrane-bound prestin. Prestin-based OHC motility is thought to be responsible for cochlear amplification, which contributes to the exquisite frequency selectivity and sensitivity of mammalian hearing. Prestin belongs to an anion transporter family, the solute carrier protein 26A (SLC26A). Prestin is unique in this family in that it functions as a voltage-dependent motor protein manifested by two hallmarks, nonlinear capacitance and motility. Evidence suggests that prestin orthologs from zebrafish and chicken are anion exchangers or transporters with no motor function. We identified a segment of 11 amino acid residues in eutherian prestin that is extremely conserved among eutherian species but highly variable among non-mammalian orthologs and SLC26A paralogs. To determine whether this sequence represents a motif that facilitates motor function in eutherian prestin, we utilized a chimeric approach by swapping corresponding residues from the zebrafish and chicken with those of gerbil. Motility and nonlinear capacitance were measured from chimeric prestin-transfected human embryonic kidney 293 cells using a voltage-clamp technique and photodiode-based displacement measurement system. We observed a gain of motor function with both of the hallmarks in the chimeric prestin without loss of transport function. Our results show, for the first time, that the substitution of a span of 11 amino acid residues confers the electrogenic anion transporters of zebrafish and chicken prestins with motor-like function. Thus, this motif represents the structural adaptation that assists gain of motor function in eutherian prestin.

Key words: Prestin, Protein motif, Electromotility, Evolution, Zebrafish

Introduction

The outer hair cell (OHC) is one of two receptor cells in the organ of Corti, and plays a crucial role in mammalian hearing. OHCs are able to rapidly change their length (Brownell et al., 1985; Kachar et al., 1986) and stiffness (He and Dallos, 1999) when their membrane potential is altered. It is generally accepted that OHC motility is responsible for amplifying low level signals in the cochlea, which ultimately contributes to the exquisite frequency selectivity and sensitivity of mammalian hearing (Liberman et al., 2002; Dallos et al., 2008). This so-called electromotility is the result of conformational changes of a membrane-bound protein named prestin (Zheng et al., 2000). Prestin belongs to a distinct anion transporter family, designated as solute carrier protein 26A, or SLC26A (Zheng et al., 2000). All the SLC26A members share two domains, one consisting of the sulfate transporter (SulpTP) domain and the other comprising the Sulphate Transporter and AntiSigma factor antagonist (STAS) domain. The SulpTP domain is a ~438 residue region that contains hydrophobic α-helical transmembrane spanning (TM) sequences (Zheng et al., 2000; Oliver et al., 2001; Navaratnam et al., 2005; Lovas et al., 2011). Members of this family serve two fundamentally distinct functions. Although most members transport different anion substrates across epithelia (Mount and Romero, 2004; Ohana et al., 2009), mammalian prestin is unique in that it functions as a voltage-dependent motor protein (Dallos and Fakler, 2002; He et al., 2006). In contrast, prestin orthologs from zebrafish and chicken are electrogenic anion exchangers or transporters with no motor function (Albert et al., 2007; Schaechinger and Oliver, 2007; Tan et al., 2011).

Short-sequence motifs, typically 5–25 amino acid residues, are often associated with evolutionary acquisition of important structural or functional characteristics of a protein (Saito et al., 2004; Saito et al., 2007). The newly derived functions are typically associated with regions of a protein that have high peptide sequence variability (Kimura, 1983). Evolutionary studies combined with comparative genomic and bioinformatic analyses have identified two regions of amino acid sequences that are highly invariant among eutherian species, but highly polymorphic among non-mammalian vertebrates and SLC26A paralogs (Franchini and Elgoyhen, 2006; Rajagopalan et al., 2006; Okoruwa et al., 2008; Elgoyhen and Franchini, 2011). Based on the fact that motor capability is an innovation of mammalian prestin, we predict that the structural innovation underlying motor function in eutherian prestin evolved from a site within the SulpTP domain that has well-conserved amino acid composition among mammalian prestins but is highly variable in non-mammalian prestin orthologs. One region of 11 amino acid residues within the SulpTP domain appears to be a newly derived, highly conserved feature for the eutherian prestin (Okoruwa et al., 2008) because insertions and deletions of amino

acids are observed in both non-mammalian orthologs and the other SLC26A paralogs. Therefore, this 11-amino-acid motif [designated herein as the Motile Eutherian SLC26A Helper (MESH) motif] represents structural innovation important for the evolution of motor capability in eutherian prestin. To test this hypothesis, we swapped corresponding residues from the zebrafish and chicken with the MESH motif from gerbil prestin. Zebrafish and chicken prestin orthologs function as anion transporters with no motor capability (He et al., 2003; Albert et al., 2007; Tan et al., 2011). A gain of motor function with the hallmarks of nonlinear capacitance (NLC) and somatic motility observed in the chimeric zebrafish and chicken prestin proteins suggests this MESH motif represents the structural adaptation that is crucial for the gain of motor function in eutherian prestin during evolution.

Results

Gain of nonlinear capacitance in chimeric prestins of zebrafish and chicken

We selected the site for investigation that encompasses residues 158–168 in gerbil prestin, representing the homologous regions in other eutherians. The amino acids in this motif are invariant among over 30 mammalian species examined (Okoruwa et al., 2008), but exhibit insertions and deletions in the non-mammalian vertebrate orthologs (see Table 1). To demonstrate that this MESH motif represents the structural adaptation that confers eutherian prestin with motor capability, chimeric prestin constructs (see Fig. 1) were developed for physiological analyses. Gerbil, zebrafish and chicken prestins were used for substitution of amino acids. Fig. 1A shows the amino acid sequences of gerbil, zebrafish and chicken prestins. The equivalent regions in gerbil, chicken and zebrafish prestin sequences were identified by amino acid sequence alignment using BLAST. The residues 158–168 (IPGGVNATNGT) from gerbil prestin were exchanged with those from either zebrafish prestin [residues 158–171 (MVNGTNSSLVVNI)] or chicken prestin [residues 158–174 (ISVGYNSTNATDASDYY)] (Fig. 1). All three chimeric prestin clones exhibited cell surface expression 24–48 hours after transfection, as evident by the membrane-associated EGFP expression (Fig. 2A). Each chimeric protein was then tested for NLC. NLC reflects voltage-dependent charge movement that arises from the redistribution of charged 'voltage sensors' across the membrane (Ashmore, 1989; Santos-Sacchi, 1991). We first measured NLC from gerbil prestin-expressing human embryonic kidney (HEK) cells and an example is shown in Fig. 2B. Gerbil prestin produced a bell-shaped response with a peak capacitance of approximately 1.2 pF at −73 mV. Four parameters (Q_{max}, C_{lin}, $V_{1/2}$ and z), that are often used to define the magnitude and voltage-dependency of NLC (Dallos and Fakler, 2002; Ashmore, 2008), were obtained from nonlinear curve-fitting of the NLC response using the first derivative of the Boltzmann function (the equation is provided in the Materials and Methods section). Q_{max} is maximum charge transfer, C_{lin} is linear capacitance, $V_{1/2}$ is the voltage at which half of the total charges are translocated across the membrane, and z is the valence of charge movement. Because HEK cells varied in size, which was reflected by the C_{lin} value, NLC and Q_{max} obtained from each cell were normalized by its C_{lin}. The normalized mean values and standard deviations of the four parameters from six gerbil prestin-expressing cells are shown in Fig. 2C. Using the same voltage protocol, we measured NLC from eight zebrafish prestin-expressing cells. As shown in Fig. 2B, a small elevated peak significantly shifted ($P<0.01$) in the direction of positive potential was observed. The response did not reach a peak even at 150 mV in most cases, and could not be determined due to membrane breakdown with large voltage stimulation. Because no clear peak was observed within the voltage applied in most cases for zebrafish prestin, no parameters were obtained for zebrafish prestin. To determine whether there was a gain of NLC in a zebrafish prestin chimera that contained residues 158–168 from gerbil prestin [chimera designated as Zf(g)], we measured NLC from Zf(g)-expressing cells. As shown in Fig. 2B, a significant gain of the magnitude of NLC was observed ($P<0.01$). Accompanying the magnitude gain, the peak response also shifted significantly ($P<0.01$) toward the negative potential. Eight Zf(g)-transfected cells were assayed and the values of means and standard deviations of the four parameters are presented in Fig. 2C.

Chicken prestin shows 58% amino-acid identity with rat prestin (Schaechinger and Oliver, 2007) and has a small NLC

Table 1. Variation in the eutherian motif of prestin among vertebrate species

Species	Common name	Sequence			
Eutherian consensus	Mammal	DDIV	IPGG-VNATNGT	------	EAR
Rattus norvegicus	Rat	DDIV	IPGG-VNATNGT	------	EAR
Meriones unguiculatus	Gerbil	DDIV	IPGG-VNATNGT	------	EAR
Monodelphis domestica	Opossum	DDMY	VGGGGANSTNGT	------	EER
Ornithorhynchus anatinus	Platypus	DDMF	-AGG-MNSTNST	------	EER
Anolis carolinensis	Anole Lizard	DEMF	-DIIDTNSTNST	YA-DNF	KAR
Gallus gallus	Chicken	DEVI	-SV-GYNSTNAT	DASDYY	SLR
Meleagris gallopavo	Turkey	DEVT	-FV-GYNSTNTT	DASDYY	SLR
Taeniopygia guttata	Zebra Finch	DEII	-SL-DSNSTNTT	DVLEYY	SAR
Xenopus tropicalis	Frog	DEMF	-DIMPANGTNST	DFDEKI	EAR
Danio rerio	Zebrafish	DSMF	M----VNGTNST	LVVN-I	EAR
Oryzias latipes	Medaka	DHMF	-PVFSGNATNNT	SVFDK-	EAC
Gasterosteus aculeatus	Stickleback	DSMF	-YVLPANGTNVT	AVLD-V	EAR

Sequence alignment is depicted with the consensus residues conserved among all SLC26A5 orthologs being underlined. The conserved mammalian residues are indicated by the gray highlighted residues. The vertical dashed lines indicate the boundaries representing the amino acids that comprise the MESH motif and the equivalent regions in the other mammalian, opossum and platypus, and the non-mammalian vertebrate species.

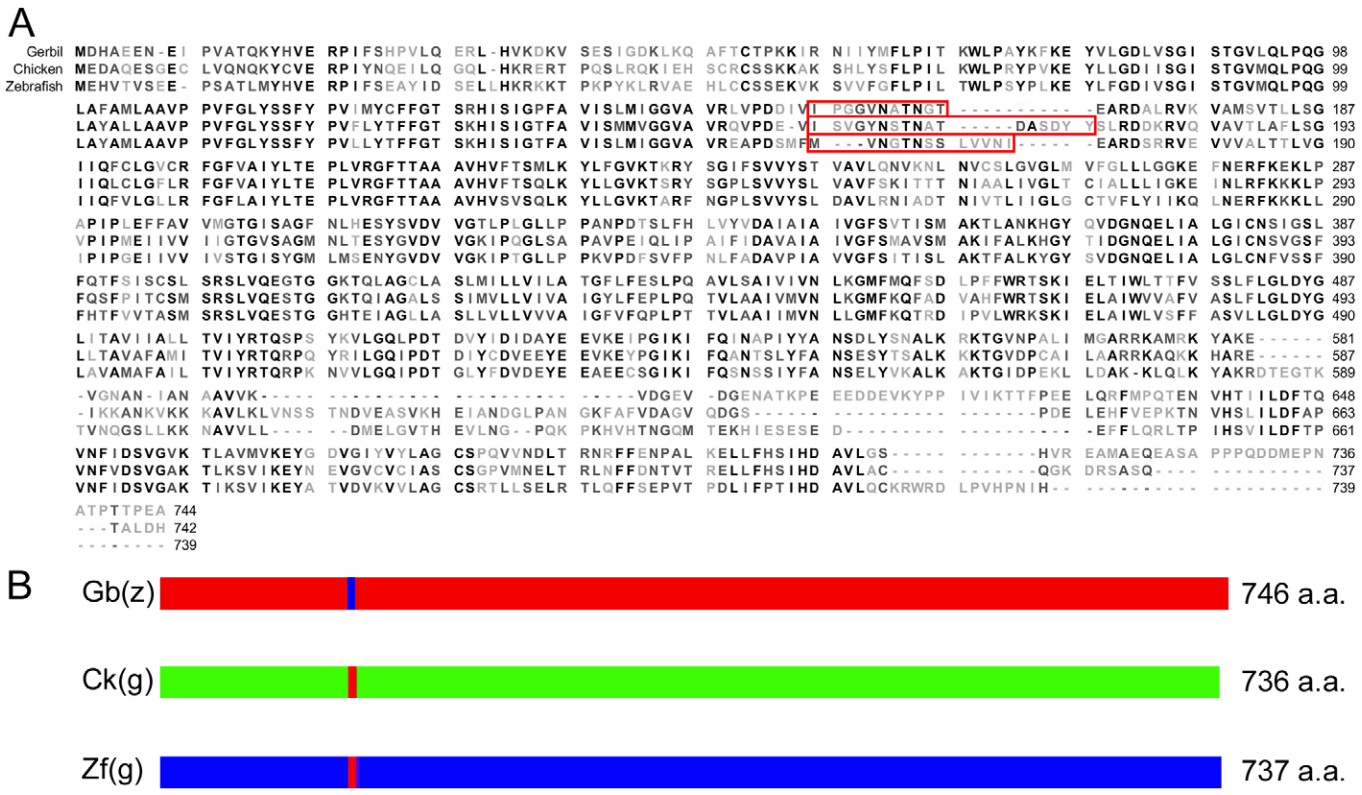

Fig. 1. *Construction of prestin chimeras containing the MESH motif and the consensus amino acid sequences of gerbil, chicken and zebrafish prestins.* (**A**) Amino acid sequences for gerbil, chicken and zebrafish prestins. Identical residues in the consensus sequences are shown in bold with the light shaded residues indicating a non-synonomous alignment. Amino acid residues marked by red lines represents the motifs that were swapped. (**B**) Scheme of the constructs of chimeric Zf(g), Ck(g) and Gb(z). The number of amino acid residues indicates the length of each chimeric protein after substitution.

with the peak significantly shifted in the positive potential (Tan et al., 2011). We attempted to demonstrate that substitution of this MESH motif could also confer chicken prestin with significant gain of NLC. We first measured NLC from chicken prestin-transfected cells (Fig. 3A). As shown in Fig. 3B, the NLC of chicken prestin exhibited a small peak significantly shifted toward the positive potentials compared to gerbil prestin ($P<0.01$). Four parameters obtained from curve fitting of the NLC response from chicken prestin-expressing cells ($n=7$) are presented in Fig. 3C. We substituted chicken prestin residues 158–176 with the gerbil prestin residues 158–168. The resulting Ck(g) chimeric protein was expressed in the membrane (Fig. 3A). Measurements of NLC from Ck(g) showed that there was a significant gain ($P<0.05$) in the magnitude of NLC after the residues were replaced. The gain of NLC was also accompanied by a shift of $V_{1/2}$ toward negative potential compared with chicken prestin.

We measured NLC from chimeric gerbil prestin with substitution of residues 158–171 from zebrafish prestin [chimera designated as Gb(z)] to determine whether there was an elimination or reduction of NLC. If residues 158–168 in gerbil prestin were important for the gain of NLC in eutherian prestin, substitution by residues from an equivalent region in zebrafish prestin would substantially reduce NLC in the chimera Gb(z). Fig. 4A shows an example of NLC measured from Gb(z). Nine Gb(z)-transfected cells were measured and compared to gerbil prestin-transfected cells. Gb(z)-transfected cells exhibited a significant reduction ($P<0.01$) in the magnitude of NLC. The reduction is accompanied by a significant shift ($P<0.01$) in $V_{1/2}$ toward the negative potential. Four parameters resulting from Boltzmann curve fitting are presented in Fig. 4B. The reduction in NLC of Gb(z) suggests that this MESH motif is important for the manifestation of NLC properties in gerbil prestin.

A prolyl residue and three glycyl residues are present in the eutherian motif and together these residues might constitute a kink with a flexible random coil. Substitutions were made to replace proline 159 with valine (P159V) and the adjacent glycine with alanine (G160A) in gerbil prestin, Zf(g) and Ck(g) to determine whether such alterations would affect the magnitude and voltage-dependency of NLC. All three mutated proteins [designated gPres(m), Zf(gm) and Ck(gm)] were expressed in the plasma membrane and exhibited NLC. As shown in Fig. 5, there was shift in $V_{1/2}$ of approximately 20 mV towards the negative potential in all three mutants. The shifts were statistically significant ($P<0.05$) in all three mutants. However, no differences were found in any of the three mutants when the magnitude of NLC was compared before and after mutation.

Gain of motor function in chimeric prestins of zebrafish and chicken

Substitution of the MESH motif from gerbil prestin significantly augmented the magnitude of NLC in Zf(g) and Ck(g). We used the microchamber technique (He et al., 1994; He, 1997; Zheng et al., 2000; Albert et al., 2007) to measure electromotility of the

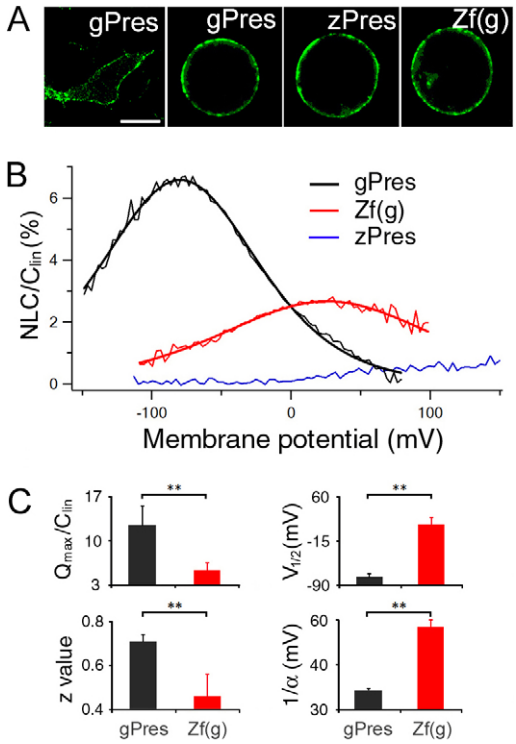

Fig. 2. Heterogenic expression and NLC of gerbil and zebrafish prestin and Zf(g). (**A**) Representative confocal images of HEK cells transfected with gPres, zPres and Zf(g). The image on the left is from an attached HEK cell and the others are from detached HEK cells, transfected with EGFP-tagged constructs. Scale bar: 10 µm. (**B**) NLC (thin traces) obtained from gPres-, zPres- and Zf(g)-transfected HEK cells. The capacitance–voltage responses of gPres and Zf(g) were fitted with the Boltzmann function (thick lines). NLC was normalized by linear capacitance (C_{lin}). (**C**) Means + s.d. of four parameters obtained from gPres (n=6) and Zf(g) (n=8) after fitting with Boltzmann function. **P<0.01 (Student's t-test).

transfected HEK cells to determine whether the gain of NLC could confer Zf(g) and Ck(g) with motor capability. An estimated voltage of ±200 mV (peak-to-peak) was applied to the extruded membrane segment. This voltage magnitude was large enough to generate saturated responses. HEK cells transfected with gerbil prestin exhibited large cycle-by-cycle response to the sinusoidal voltage stimulation (Fig. 6A). The magnitude of the motile response was 85±27 nm (mean ± s.d., n=8). We also measured motility from HEK cells transfected by zebrafish or chicken prestin. No signs of time-registered and stimulus-following responses were detected in any of the cells transfected with zebrafish or chicken prestin (n=9 and 7 for zebrafish and chicken prestin, respectively) measured with a system resolution of 5 nm. Examples of lack of motility are presented in Fig. 6. We used the same voltage protocol to measure motility from eight Zf(g)- and six Ck(g)-expressing cells. Cycle-by-cycle responses to the sinusoidal voltage stimulus were observed in both Zf(g)- and Ck(g)-transfected cells (Fig. 6). The magnitude of motility was 33±9 nm for Zf(g) and 57±13 nm for Ck(g), both being significantly less than that of gerbil prestin-transfected cells (P<0.01). This was not surprising because the magnitude of NLC in Zf(g) and Ck(g) was also significantly less than that of gerbil prestin. However, the gain of motility in Zf(g) and Ck(g) clearly correlated with the enlargement of NLC seen in these chimeric proteins.

We also measured the motile response from Gb(z) to determine whether there was a significant reduction of motility. If the MESH motif is important for motor function in prestin, then substituting it with 13 amino acids from the corresponding region of zebrafish prestin would substantially reduce motility in Gb(z). We measured five Gb(z)-transfected cells. An example is depicted in Fig. 6. Gb(z)-transfected cells still retained some cycle-by-cycle responses with a magnitude of 23±8 nm (n=5). By contrast, the motile response of gerbil prestin was 85±27 nm (n=8). Thus, substitution of the MESH motif with 13 amino acids from zebrafish prestin caused a 73% reduction of the motility magnitude seen in Gb(z).

Transport function of chimeric prestin is retained

Because prestin orthologs from zebrafish and chicken demonstrate the ability to transport anions (Schaechinger and Oliver, 2007), we wanted to find out whether the substitution affects the structure underlying transport capability. In other words, whether the gain of motor function in Zf(g) and Ck(g) was at the expense of transport function? We measured anion transport capability by using standard radioactive-labeled formate uptake assays (Bai et al., 2009; Tan et al., 2011). Pendrin (human), a paralog of prestin, was used as a positive control (Tan et al., 2011). The vector carrying EGFP was used as a negative control. HEK cells transfected with human pendrin showed a robust formate-transport capability with an increase of ~300% (140±17 pmol) compared to the EGFP control (47±3 pmol) (Fig. 7). Formate-transport capability of zebrafish and chicken prestin also showed a significant increase above control levels (P<0.01 and P<0.05, respectively). Cells transfected with gerbil prestin did not show a significant increase relative to the control. This is consistent with a previous study (Tan et al., 2011). The formate uptake of Zf(g) and Ck(g) were also significantly greater than the EGFP-transfected control (P<0.01 and P<0.05, respectively). Comparisons between Zf(g) and zebrafish prestin, as well as between Ck(g) and chicken prestin, showed that formate uptake was not statistically different in either group (P>0.05), suggesting that the transport activities of zebrafish and chicken prestins were unaffected by swapping of this motif.

We also measured the formate uptake of Gb(z) to determine whether Gb(z) had acquired transport capability. As shown in Fig. 7, formate uptake of Gb(z) was not statistically different from that of gerbil prestin. Thus, this 13-amino-acid motif in zebrafish prestin does not appear to be the structural factor important for transport function.

Discussion

We showed that the swapping of a span of 11 amino acid residues confers the electrogenic anion transporters of zebrafish and chicken prestin orthologs with motor function. This is the first time it has been demonstrated that a substitution of 11 amino acid residues, the MESH motif, is sufficient to confer zebrafish and chicken prestin orthologs with prestin-like capabilities, regardless of the orthologous protein context within which it is placed. As further proof of principle, we were able to confer prestin's motor-like property into human pendrin by swapping of the mammalian MESH motif (Tan et al., 2011). Furthermore, the Gb(z) chimera with the MESH motif replaced by 13 amino acids

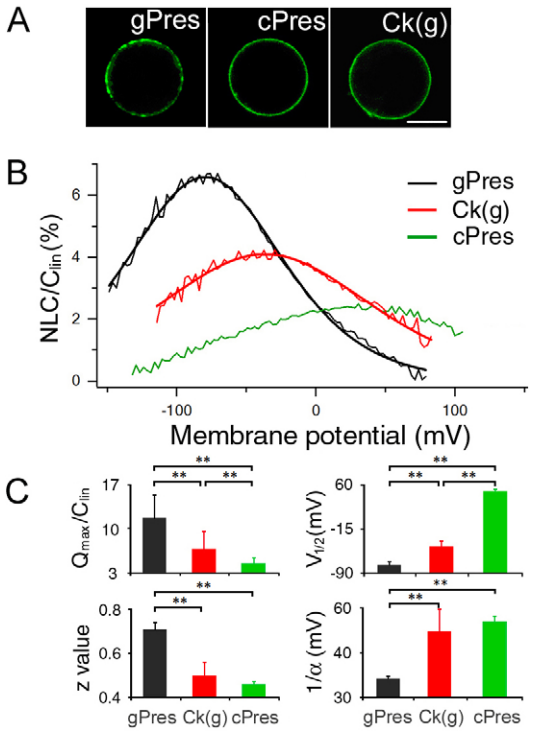

Fig. 3. Heterogenic expression and NLC of gerbil and chicken prestin and Ck(g). (**A**) Confocal images of detached HEK cells transfected with gPres, cPres and Ck(g). Scale bar: 10 µm. (**B**) NLC obtained from gPres-, cPres- and Ck(g)-transfected HEK cells. Thick lines represent curve fitting using the Boltzmann function. (**C**) Means + s.d. of four parameters obtained from Boltzmann function for gPres (n=6), cPres (n=7) and Ck(g) (n=7). **P<0.01 (Student's t-test).

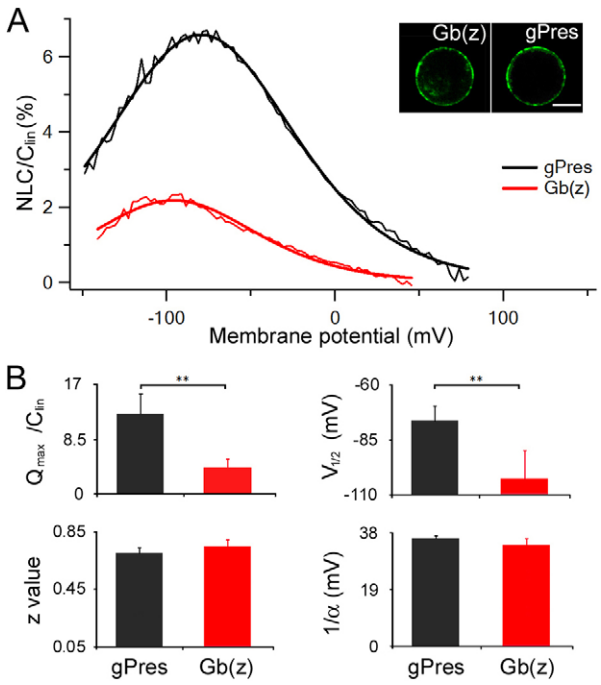

Fig. 4. Heterogenic expression and NLC of gerbil prestin and Gb(z) containing 13 amino acid residues from zebrafish prestin. (**A**) NLC obtained from gPres- (n=6) and Gb(z)-transfected (n=9) HEK cells. The insets show confocal images of detached gPres- and Gb(z)-transfected HEK cells. Scale bar: 10 µm. The capacitance–voltage responses (thin traces) were fitted with the Boltzmann function (thick lines). (**B**) Four parameters derived from curve fittings with Boltzmann's function. Data are expressed as mean ± s.d. **P<0.01 (Student's t-test).

from the equivalent region from zebrafish prestin showed a significant reduction of NLC. On the basis of our findings, we propose that the MESH motif represents the structural adaptation that is important for the gain of motor function in prestin. Although the two chimeric prestin orthologs were reduced in length by two residues in Zf(g) and six residues in Ck(g), the cell membrane localization and anion transport capability were not altered. The fact that the gain of motor function is not accompanied by loss of transport function implies that the molecular structures underlying the motor and transport properties of the chimeric proteins, Zf(g) and Ck(g), are separated. This is in contrast to a recent study that suggested that prestin-based electromotility is a dual-step process mediated by the transport of monovalent anions (Schaechinger et al., 2011). However, our conclusion is consistent with an earlier study that suggested that motor and transport activity are independent (Bai et al., 2009). The inability of the MESH motif to influence transport function in the Zf(g) and Ck(g) chimeras also supports the notion that this peptide stretch was accessible for evolutionary changes and subsequent divergence from the non-mammalian vertebrates. We noted that the magnitude of NLC and motility of Zf(g) or Ck(g) was still significantly less than that of gerbil prestin. This is not surprising because the amino acid sequences, and perhaps the associated secondary and tertiary structures of eutherian prestin and non-mammalian prestin orthologs, are different. It is conceivable that the full expression of motor function would require additional regions and/or structures in the molecule to work together.

Questions might be raised as to whether the gain of NLC in Zf(g) or Ck(g) is the result of increased level of membrane expression of the chimeric proteins, as an effect of the substitution of the gerbil prestin peptide. In order to minimize this possibility, great care was taken to identify and record from transfected cells with similar-appearing intensities of EGFP fluorescence in the membrane. This should be useful to minimize variation between different cells and constructs. Use of such an approach for cell selection represents the current standard for profiling the electrophysiological properties of prestin in transfected cells. Currently, no technically feasible and reliable (i.e. sensitive enough) methodologies are available to quantify membrane protein expression for individual cells during electrophysiological recording. Although we cannot quantify the level of membrane expression in different cells, increased level of membrane expression of Zf(g) or Ck(g) is inconsistent with our findings. The main reason to argue against such possibility is that the significant gain of NLC is also accompanied by a significant shift of $V_{1/2}$ in both Zf(g) and Ck(g). An increase of prestin expression in the membrane might result in an enlargement in the magnitude of NLC, but should not cause a shift of voltage dependency (Seymour et al., 2011). In addition, the gain of NLC is accompanied by a gain of somatic motility. The expression of a protein with no motor capability in the membrane will not generate somatic motility, regardless of how densely the protein is expressed. It is, therefore, conceivable that the significant gain of

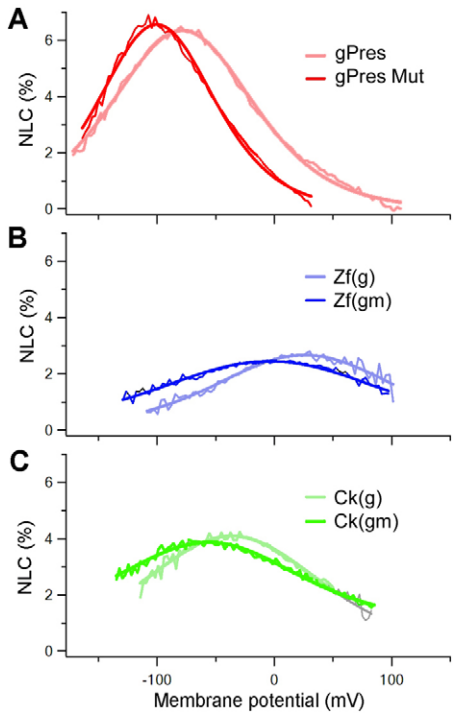

Fig. 5. NLC after point mutations. (**A**) NLC obtained from gPres and gPres with P159V and G160A mutations (gPres Mut). (**B**) NLC responses from Zf(g) and Zf(g) with P159V and G160A mutations [Zf(gm)]. (**C**) NLC responses from Ck(g) and Ck(g) with P159V and G160A mutations [Ck(gm)]. Thin traces indicate the NLC response and thick lines represent the corresponding Boltzmann fitting.

NLC is not due to improvement of membrane targeting for Zf(g) and Ck(g). During functional evolution of prestin from zebrafish to gerbil, NLC becomes more prominent, along with a characteristic shift of $V_{1/2}$ from positive to negative potentials (Tan et al., 2011; Izumi et al., 2011). The shift in voltage dependency after substitution correlates with the trend of $V_{1/2}$ shift during evolutionary transition from non-mammals to mammals, when gain of motor function of prestin is first observed in the prototherian (platypus) species (Tan et al., 2011).

We observed acquisition of somatic motility in Zf(g) and Ck(g). It has been reported that transmembrane voltage can modulate membrane tension to create a state of flexoelectricity, which can result in membrane movement even in nontransfected or tethered HEK cells (Zhang et al., 2001; Brownell et al., 2010). The amplitude of such tension-based membrane motion depends on the ionic strength in the solution and is proportional to voltage, with conversion efficiency of about 1 nm per 100 mV. With such low conversion efficiency, the total length change of the non-transfected HEK cells would only correspond to about 4 nm (if ±200 mV was applied to the cell segment). Such membrane motility (Zhang et al., 2001), if any, was below the 5-nm resolution limit of our measurement system. The motion observed from Zf(g) and Ck(g) is, however, at least ten times greater than the tension-based motility. Therefore, the gain of somatic motility in Zf(g) or Ck(g) was not an artifact related to the tension-based membrane motility.

Schaechinger and colleagues recently reported that a zebrafish prestin containing substitutions of two different sites from rat prestin rendered the chimeric protein with motor capability (Schaechinger et al., 2011). These two fragments were represented by rat prestin amino acid residues 86–140 and 381–438. Approximately 26% (113/438) of the SulpTP domain residues were exchanged from the rat into the zebrafish prestin. NLC was only observed when both rat prestin regions were included in the zebrafish chimera. In contrast, chimeric zebrafish prestins with either region alone exhibited properties similar to those of zebrafish prestin. The first region encompasses the SLC26A transporters signature pattern (residues 109–130, Prosite PS01130) and is conserved among all SLC26A members (Zheng et al., 2000). The second region putatively includes two hydrophobic α-helices, representing TM domains 9 and 10 in the 12 TM model (Oliver et al., 2001; Dallos and Fakler, 2002). Comparisons of the rat and zebrafish prestin amino acid sequences show an alignment where the identical (identity) or common replacement (positive) residues display 87% (48/55) identity and 98% (54/55) positive for the first region and 57% (33/58) identity and 78% positive (45/58) for the second region. Of the non-synomonous amino acids, only one residue (P124) in region 1 and four residues (S383, S392, C395 and C415) in region 2 were non-conserved substitutions, based on point accepted mutation 250 (PAM250) log-odds matrix scores. It is, therefore, difficult to comprehend why and how these five amino acids, scattered in these two regions, could be responsible for the gain of motor function in their zebrafish prestin chimera. By contrast, we predict that the structure(s) responsible for the evolution of motor capability should lie in a region(s) that is new and conserved in mammalian prestin, but is highly variable in the non-mammalian vertebrate prestin orthologs. The structural basis of innovation of motor capability in mammalian prestin should reflect the functional changes in the SLC26A transporter to acquire motile properties. Apparently, the present study and the study of Schaechinger et al. (Schaechinger et al., 2011) were fundamentally different in the way in which the areas (structures) were identified. At present, it is difficult to reconcile our conclusion with that of Schaechinger et al. (Schaechinger et al., 2011). However, it is possible that there might be several areas in the prestin molecule that facilitate, in toto, the maximum gain of motor function.

Based on the acquisition of NLC and motor-like activities in Ck(g) and Zf(g), the mechanism by which the eutherian motif elicits the acquisition of these properties is not clear. It is conceivable that both length and amino acid composition of the MESH motif contribute to the acquisition of motor function. We deduced this from our experimental data and comparative sequence alignments (Table 1). One of the significant deletions during the evolution of mammalian prestin is the deletion of five or six residues at the carboxyl end of this segment (Okoruwa et al., 2008). It appears that 10–12 residues is the length constraint at this site for motor function because most of the other non-mammalian vertebrate prestin orthologs exhibited sizes of 16–17 residues at this site. This peptide stretch is 10 residues in the prototherian platypus and 12 amino acids in the metatherian opossum. Demonstration of NLC and motility in platypus (Tan et al., 2011; Izumi et al., 2011) and opossum (our unpublished data) implies that variation of 10–12 residues at this site is feasible. Residue composition also appears to be an important prerequisite. As shown in Table 1, there is a segment after the IPGGV (158–162) where the majority of amino acids (six residues, NATNGT, 163–168) are common to the different vertebrate species. The

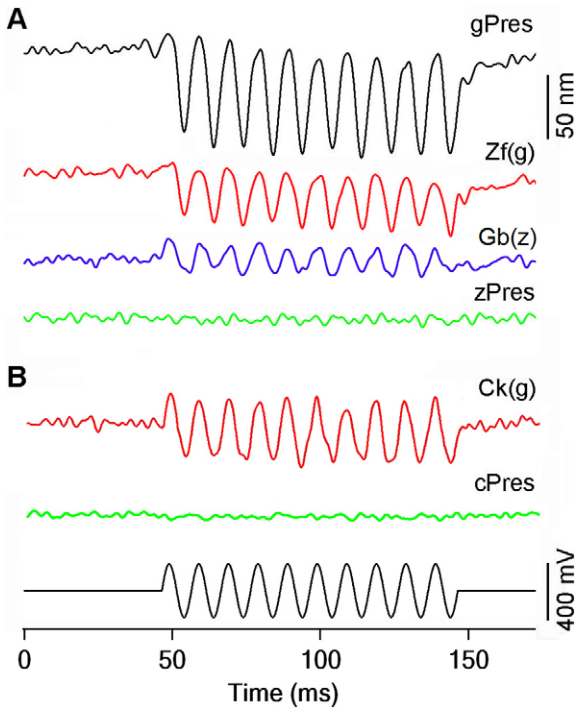

Fig. 6. Motility measured from prestin and chimeric proteins. (**A**) Examples of motile responses measured from HEK cells transfected with gPres, Zf(g), zPres or Gb(z). (**B**) Examples of motility responses measured from Ck(g)- and cPres-transfected HEK cells. The responses were the results of 200 averages. The electrical stimulus (bottom panel) was a 100-Hz sinusoidal voltage burst with duration of 100 milliseconds. The estimated voltage drop on the extruded segment varied from −200 to 200 mV.

substitution of a glycyl residue (G167) within this stretch is fixed within the eutherian motif and is probably another adaptive feature. The contribution of G167 still needs to be ascertained. The IPGGV (158–162) peptide is present in the eutherian orthologs with the PGG peptide, providing a different configuration to the equivalent segment in non-mammalian orthologs. Both platypus and opossum have glycyl residues in these positions, but lacked the eutherian-derived proline. The mutational data suggest that the composition of glycyl and prolyl residues per se did not appear to

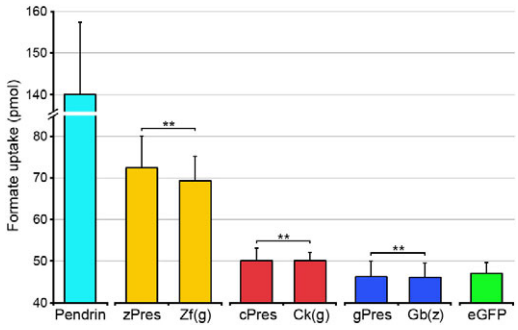

Fig. 7. Formate uptake by HEK cells transfected with prestin orthologs and chimeras. Human pendrin was used as a positive control and the pEGFP vector was used as a negative control. Means + s.d. (n=9 for each construct). **P<0.05 (Student's t-test).

be crucial for the gain of NLC. With recent inclusion of protein sequences from echolocating bat and whale species (Li et al., 2008; Li et al., 2010), SLC26A5 peptide sequences are now available from over 50 eutherian species. Polymorphisms are observed adjacent to eutherian motif in some of the echolocating species.

Most of the current topological models of the SLC26A sequences, including mammalian prestin, feature a SulpTP core domain comprising of 10 or 12 TM regions (Oliver et al., 2001; Dallos and Fakler, 2002; Mount and Romero, 2004; Navaratnam et al., 2005; Dossena et al., 2009). In these models, the MESH motif is outside of the predicted α-helical hydrophobic TM spanning regions and is within a predicted hydrophilic loop. The motif is located within the second extracellular loop in the 12 TM model (Oliver et al., 2001; Deak et al., 2005) and is the first intracellular loop in the 10 TM model (Navaratnam et al., 2005). On the basis of these topological models, it was surprising that the MESH motif could elicit the gain of function observed in the chimeric zebrafish and chicken prestin proteins. Interestingly, two putative N-glycosylation (N163 and N166) sites were identified within the MESH motif, as predicted by the 12 TM model. These two asparagines are highly conserved within the SLC26A family (Matsuda et al., 2004). There are conflicting reports about whether or not these two sites are actually glycosylated in prestin (Matsuda et al., 2004; Navaratnam et al., 2005; Rajagopalan et al., 2010). Cell surface expression is unaffected by substitution of both asparagines with alanine residues, and these mutant proteins exhibited only minor alterations in their physiological properties (Matsuda et al., 2004; Navaratnam et al., 2005; Rajagopalan et al., 2010; Azroyan et al., 2011). However, recent evidence demonstrated that the mouse Slc26A4 paralog, pendrin, is glycosylated at the equivalent sites (N167 and N172) (Azroyan et al., 2011). Undoubtedly, these models are inadequate to explain the contribution of the MESH motif to the conformational changes of prestrin from the compact to expanded state, with membrane potential determining the probability of each conformation (Oliver et al., 2001; Dallos and Fakler, 2002). In fact, structure–function correlations of the whole SLC26A family are poorly understood, with conflicting topological models. We have recently determined the three-dimensional (3D) structure of the SulpTP domain of rat prestin by combining ab initio structure prediction, 3D folding recognition by threading, homology modelling and molecular dynamics simulations. Our results suggest that the MESH motif is in the first intracellular loop (Lovas et al., 2011). Therefore, the MESH motif most likely facilitates and translates the internal charge movement into expansion and contraction of the molecule, which ultimately promotes somatic motility at a microsecond time scale. Understanding how this MESH motif facilitates motor function ultimately depends on the full elucidation of the 3D structure of prestin. The present identification of the crucial amino acid sequence represents the first of many required steps towards a mechanistic understanding of how prestin works.

In conclusion, we have identified a small fragment that represents one of the key adaptive structures in the eutherian prestin. This motif is capable of conferring motor-like properties to non-mammalian vertebrate prestin orthologs without disrupting their transport capabilities. Studies are ongoing to investigate the length and sequence constraints of this eutherian motif in motor function.

Materials and Methods

Swapping of the 11-amino-acid fragment

Gerbil (*Meriones unguiculatus*), chicken (*Gallus gallus*) and zebrafish (*Danio rerio*) prestin cDNAs (courtesy of Dominik Oliver, Philipps University, Marburg, Germany) were cloned into the pEGFP-N1 vector to generate the C-terminal EGFP fusion proteins. Amino acids 158–168 of gerbil prestin were defined as a site exhibiting considerable diversity between mammals and non-mammalian vertebrates (Okoruwa et al., 2008) and the equivalent regions in gerbil and zebrafish prestin sequences were identified by amino acid sequence alignment. The residues from the gerbil (residues 158–168, IPGGVNATNGT) were exchanged with those from either zebrafish (residues 158–171, MVNGTNSSLVVNI) or chicken (residues 158–174, ISVGYNSTNATDASDYY) (Fig. 1) to create the chimeras Zf(g) and Ck(g), respectively. Chimera mutants were constructed by swapping this site into cDNA fragments that were flanked by unique restriction enzyme sites specific for cDNAs from each species. These fragments were synthesized and cloned into the pUC57 vector (GenScript, Piscataway, NJ). Chimeric cDNAs were produced by digestion of the orthologs from gerbil, chicken and zebrafish and then re-ligated to incorporate the chimeric cDNA fragments to generate EGFP fusion proteins. As shown in Fig. 1, the zebrafish Zf(g) or chicken Ck(g) prestin chimeras were constructed with the gerbil site being swapped. A third chimera had the zebrafish fragment substituted into gerbil prestin to create a Gb(z) prestin protein. Additional prestin clones were produced by site mutagenesis, performed using the QuikChange Lighting site-directed mutagenesis kit (Stratagene, La Jolla, CA), where two residues, P159V and G160A, in the motility motif were substituted in gerbil prestin [gPres(m)], in chicken chimera [Ck(gm)] and in zebrafish chimera [Zf(gm)].

The three oligonucleotide sets were as follows: gerbil, forward 5′-TCGTCATCGTGGCAGGAGTGAACGCAACC-3′ and reverse 5′-GGTTGCGT-TCACTCCGCCACGATGACGATGTCATCG-3′; Ck(g), forward 5′-GCCTGA-TGAAGTGATCGTGGCAGGAGTGAACGCAACC-3′ and reverse 5′-GGTTGC-GTTCACTCCTGCCACGATCACTTCATCAGGC-3′; and Zf(g), forward 5′-CCCCAGACTCCATGTTTATCGTGGCAGGAGTGAACGCAA-3′ and reverse 5′-TTGCGTTCACTCCTGCCACGATAAACATGGAGTCTGGGG-3′. The correct orientation, reading frame and amino acid composition of all the constructs were confirmed by sequence analyses.

Cell culture and transient transfection

HEK cells were cultured in the attached condition in DMEM solution (Invitrogen, Carlsbad, CA), supplemented with 10% fetal bovine serum. Prestin or mutants (4 μg) were introduced into the dishes using 10 μl lipofectamine (Invitrogen, Carlsbad, CA) following the protocol from the manufacturer.

Confocal imaging

Membrane-associated expression of prestin mutations was verified 24 hours after transfection by confocal imaging, performed on LSM 510 microscope (Zeiss, Thornwood, New York) using a 40× water immersion objective.

NLC measurements

NLC measurements using whole cell patch clamp techniques were performed 24–48 hours after transfection on cells with robust membrane-associated EGFP expression. Before electrophysiological recordings, HEK cells were detached and separated with trypsin (Invitrogen) treatment. The detached cells were then bathed in the extracellular solution containing 120 mM NaCl, 2 mM $MgCl_2$, 2 mM $CoCl_2$, 20 mM TEA, 10 mM HEPES and 10 mM 4-AP. Recording pipettes were pulled from borosilicate glass with resistances of 2.5–5.0 MΩ and filled with a solution containing 140 mM CsCl, 2 mM $MgCl_2$, 10 mM EGTA and 10 mM HEPES. Membrane capacitance was measured using a two-sine-wave voltage stimulus protocol (10 mV peak at both 390.6 and 781.2 Hz) with subsequent fast Fourier transform-based admittance analysis (Santos-Sacchi et al., 2001) from a holding potential of 0 mV. The capacitive currents were sampled at 100 kHz and low-pass filtered at 5 kHz. Series resistance was compensated off-line. The capacitive currents were amplified by Axopatch 200B (Molecular Devices, Sunnyvale, CA). Data were acquired using jClamp (Scisoft, New Haven, CT) and analyzed with Igor (WaveMetrics, Portland, OR).

The NLC can be described as the first derivative of a two-state Boltzmann function relating nonlinear charge movement to voltage (Ashmore, 1989; Santos-Sacchi, 1991). The capacitance function is described as:

$$C_m = C_{lin} + \frac{Q_{\max}\alpha}{\exp[\alpha(V_m - V_{1/2})](1+\exp[-\alpha(V_m - V_{1/2})])^2}$$

where, $Q_{\max}$ is maximum charge transfer, $V_{1/2}$ is the voltage at which the maximum charge is equally distributed across the membrane or, equivalently, the peak of the voltage-dependent capacitance, C_{lin} is linear capacitance and α is the slope of the voltage dependence of charge transfer. α is given by $\alpha = ze/kT$, where k is Boltzmann's constant, T is absolute temperature, z is valence of charge movement and e is electron charge. The $Q_{\max}$ was normalized by C_{lin} in the results. The C_{lin} is proportional to the surface area of the membrane (the size of the cell). Because C_{lin} is not relevant to this study, we subtracted the linear capacitance and only presented the NLC as a function of voltage for the data presented in the Results section. To compare the magnitude of NLC obtained from different cells with different sizes, we normalized the NLC by C_{lin}. Data were collected from cells whose membrane resistance were greater than 300 ΩM after rupturing and exhibited normal C_{m} and R_{m} values. Series resistance was compensated offline. For each construct, NLC data were acquired from cells representing at least four separate transfection experiments.

Motility measurements

Somatic motility of the transfected HEK cells was measured and calibrated using a photodiode-based system (He et al., 1994; Zheng et al., 2000). To measure electromotility of transfected HEK cells, a suction pipette or microchamber was used to mechanically hold the cell and to deliver voltage commands. Microchambers were fabricated from 1.5-mm thin-wall glass tubes (World Precision Instruments, Sarasota, FL). The microchamber had a series resistance of approximately 0.3–0.4 MΩ. When the cell was 50% inserted into the microchamber, the input resistance was 3-4 MΩ. The electrical stimulus was a 100-Hz sinusoidal voltage burst of 100 milliseconds in duration. Voltage commands of 400 mV (peak-to-peak) were used. Because the cells were approximately 50% inserted into the microchamber, the resultant voltage drops on the extruded segment were estimated to be 50% of the voltage applied, or 200 mV (Dallos et al., 1991; He et al., 1994). The photodiode system had a cutoff (3 dB) frequency of 1100 Hz. The sampling frequency was 5 kHz. With an averaging of 200 trials and low-pass filtering set at 200 Hz, cellular motion values as low as 5 nm could be detected.

Transporter function assessment

To measure the transport function of prestin orthologs, a conventional radioisotope technique was used. We first applied fluorescence-activated flow cytometry (FACS) to obtain EGFP-positive cells before [^{14}C]formate uptake was measured. Details for cell sorting and format uptake measurements are provided elsewhere (Tan et al., 2011; Bai et al., 2009). Pendrin and EGFP-only vector (pEGFP) were used as the positive and negative controls, respectively. Transport capabilities of the gerbil, chicken and zebrafish prestins and of the Zf(g) and Ck(g) chimeric proteins were examined. To measure [^{14}C]formate uptake, cells in the 24-well culture cluster were first incubated for 30 minutes in 130 mM NaCl, 20 mM HEPES, 5 mM KCl, 5 mM glucose, 2 mM $CaCl_2$ and 1 mM $MgCl_2$ (pH 7.3 and 305 Osm/l). Cells were then incubated at room temperature for 12 minutes 140 mM potassium gluconate, 20 mM HEPES and 5 mM glucose (pH 7.3 and 305 Osm/l). [^{14}C]formate was added to this solution to a final concentration of 20 μM. Cells were then washed three times with the cold potassium gluconate solution without [^{14}C]formate. Cells were lysed with 200 μl 0.5 M NaOH, and neutralized with 0.5 M HCl. The lysate was used for the liquid scintillation counting to determine the [^{14}C]formate uptake. The concentration (in picomoles) of the [^{14}C]-labeled formate was determined from each well estimated to contain approximately 200,000 cells. In each run, three wells were assayed for each plasmid. The experiments were repeated in three separate runs. Therefore, the data in each group were collected from a sample size (n) of nine trials for each plasmid and control.

Acknowledgements

The research described in this manuscript is part of PhD research project of X.T.

Funding

This work was supported by National Institutes of Health grants from the National Institute on Deafness and Other Communication Disorders (NIDCD) [grant numbers R01 DC008649 to K.W.B., R01 DC004696 to D.Z.Z.H.] and from the Institutional Development Award Networks of Biomedical Research Excellence (INBRE) [grant number P20 RR016469 to S.L.]. The Integrated Biological Imaging Facility, supported by the Creighton University School of Medicine, was constructed with support from the National Institutes of Health National Center for Research Resources (NCRR) [grant number C06 RR17417-01]. Deposited in PMC for release after 12 months.

References

Albert, J. T., Winter, H., Schaechinger, T. J., Weber, T., Wang., X., He, D. Z., Hendrich, O., Geisler, H. S., Zimmermann, U. and Oelmann, K. (2007). Voltage-sensitive prestin orthologue expressed in zebrafish hair cells. *J. Physiol.* **580**, 451-461.

Ashmore, J. F. (1989). *Transducer motor coupling in cochear outer hair cells: Cochlear Mechanisms* (ed. J. P. Wilson and D. T. Kemp), pp. 107-114. New York: Plenum Press.
Ashmore, J. F. (2008). Cochlear outer hair cell motility. *Physiol. Rev*. **88**, 173-210.
Azroyan, A., Laghmani, K., Crambert, G., Mordasini, D., Doucet, A. and Edwards, A. (2011). Regulation of pendrin by pH: dependence on glycosylation. *Biochem. J.* **434**, 61-72.
Bai, J. P., Surguchev, A., Montoya, S., Aronson, P. S., Santos-Sacchi, J. and Navaratnam, D. (2009). Prestin's anion transport and voltage-sensing capabilities are independent. *Biophys. J.* **96**, 3179-3186.
Brownell, W. E., Bader, C. R., Bertrand, D. and de Ribaupierre, Y. (1985). Evoked mechanical responses of isolated cochlear outer hair cells. *Science* **227**, 194-196.
Brownell, W. E., Qian, F. and Anvari, B. (2010). Cell membrane tethers generate mechanical force in response to electrical stimulation. *Biophys. J.* **99**, 845-852.
Dallos, P. and Fakler, B. (2002). Prestin, a new type of motor protein. *Nat. Rev. Mol. Cell Biol.* **3**, 104-111.
Dallos, P., Evans, B. N. and Hallworth, R. (1991). Nature of the motor element in electrokinetic shape changes of cochlear outer hair cells. *Nature* **350**, 155-157.
Dallos, P., Wu, X., Cheatham, M. A., Gao, J., Zheng, J., Anderson, C. T., Jia, S., Wang, X., Cheng, W. H., Sengupta, S. et al. (2008). Prestin-based outer hair cell motility is necessary for mammalian cochlear amplification. *Neuron* **58**, 333-339.
Deak, L., Zheng, J., Orem, A., Du, G. G., Aguinaga, S., Matsuda, K. and Dallos, P. (2005). Effects of cyclic nucleotides on the function of prestin. *J. Physiol.* **563**, 483-496.
Dossena, S., Rodighiero, S., Vezzoli, V., Nofziger, C., Salvioni, E., Boccazzi, M., Grabmighter, E., Botta, G., Meyer, G., Fugazzola, L. et al. (2009). Functional characterization of wild-type and mutated pendrin (SLC26A4), the anion transporter involved in Pendred syndrome. *J. Mol. Endocrinol.* **43**, 93-103.
Elgoyhen, A. B. and Franchini, L. F. (2011). Prestin and the cholinergic receptor of hair cells: positively-selected proteins in mammals. *Hear. Res.* **273**, 100-108.
Franchini, L. F. and Elgoyhen, A. B. (2006). Adaptive evolution in mammalian proteins involved in cochlear outer hair cell electromotility. *Mol. Phylogenet. Evol*. **41**, 622-635.
He, D. Z. (1997). Relationship between the development of outer hair cell electromotility and efferent innervation: a study in cultured organ of corti of neonatal gerbils. *J. Neurosci.* **17**, 3634-3643.
He, D. Z. and Dallos, P. (1999). Somatic stiffness of cochlear outer hair cells is voltage-dependent. *Proc. Natl. Acad. Sci. USA* **96**, 8223-8228.
He, D. Z., Evans, B. N. and Dallos, P. (1994). First appearance and development of electromotility in neonatal gerbil outer hair cells. *Hear. Res.* **78**, 77-90.
He, D. Z., Beisel, K. W., Chen, L., Ding, D. L., Fritzsch, B. and Salvi, R. (2003). Chick hair cells do not exhibit voltage-dependent somatic motility. *J. Physiol.* **546**, 511-520.
He, D. Z., Zheng, J., Kalinec, F., Kakehata, S. and Santos-Sacchi, J. (2006). Tuning in to the amazing outer hair cell: membrane wizardry with a twist and shout. *J. Membr. Biol.* **209**, 119-134.
Izumi, C., Bird, J. E. and Iwasa, K. H. (2011). Membrane thickness sensitivity of prestin orthologs: the evolution of a piezoelectric protein. *Biophys. J.* **100**, 2614-2622.
Kachar, B., Brownell, W. E., Altschuler, R. and Fex, J. (1986). Electrokinetic shape changes of cochlear outer hair cells. *Nature* **322**, 365-368.
Kimura, M. (1983). *The Neutral Theory of Molecular Evolution*. Cambridge, UK: Cambridge University Press.
Li, G., Wang, J., Rossiter, S. J., Jones, G., Cotton, J. A. and Zhang, S. (2008). The hearing gene Prestin reunites echolocating bats. *Proc. Natl. Acad. Sci. USA* **105**, 13959-13964.
Li, Y., Liu, Z., Shi, P. and Zhang, J. (2010). The hearing gene Prestin unites echolocating bats and whales. *Curr. Biol.* **20**, R55-R56.
Liberman, M. C., Gao, J., He, D. Z., Wu, X., Jia, S. and Zuo, J. (2002). Prestin is required for electromotility of the outer hair cell and for the cochlear amplifier. *Nature* **419**, 300-304.
Lovas, S., He, D. Z., Hatfield, M. P. D., Pecka, J. L., Okoruwa, O. E., Tang, J., Jia, S. P. and Beisel, K. W. (2011). *The structural features which explain the function of prestin.* Building Bridges, Proceedings of the 22nd American Peptide Symposium. (ed. M. Lebl), pp. 120-121. San Diego: Prompt Scientific Pub.
Matsuda, K., Zheng, J., Du, G.-G., Klocker, N., Madison, L. D. and Dallos, P. (2004). N-linked glycosylation sites of the motor protein: effects on membrane targeting and electrophysiological function. *J. Neurochem.* **89**, 928-938.
Mount, D. B. and Romero, M. F. (2004). The SLC26 gene family of multifunctional anion exchangers. *Pflügers Arch.* **447**, 710-721.
Navaratnam, D., Bai, J. P., Samaranayake, H. and Santos-Sacchi, J. (2005). N-terminal-mediated homomultimerization of prestin, the outer hair cell motor protein. *Biophys. J*. **89**, 3345-3352.
Ohana, E., Yang, D., Shcheynikov, N., Muallem, S. (2009). Diverse transport modes by the solute carrier 26 family of anion transporters. *J. Physiol*. **587**, 2179-2185.
Okoruwa, O. E., Weston, M. D., Sanjeevi, D. C., Millemon, A. R., Fritzsch, B., Hallworth, R. and Beisel, K. W. (2008). Evolutionary insights into the unique electromotility motor of mammalian outer hair cells. *Evol. Dev.* **10**, 300-315.
Oliver, D., He, D. Z., Klocker, N., Ludwig, J., Schulte, U., Waldegger, S., Ruppersberg, J. P., Dallos, P. and Fakler, B. (2001). Intracellular anions as the voltage sensor of prestin, the outer hair cell motor protein. *Science* **292**, 2340-2343.
Rajagopalan, L., Patel, N., Madabushi, S., Goddard, J. A., Anjan, V., Lin, F., Shope, C., Farrell, B., Lichtarge, O., Davidson, A. L., Brownell, W. E. and Pereira, F. A. (2006). Essential helix interactions in the anion transporter domain of prestin revealed by evolutionary trace analysis. *J. Neurosci.* **26**, 12727-12734.
Rajagopalan, L., Organ-Darling, L. E., Liu, H., Davidson, A. L., Raphael, R. M., Brownell, W. E, Pereira, F. A. (2010). Glycosylation regulates prestin cellular activity. *JARO* **11**, 39-51.
Saito, H., Honma, T., Minamisawa, T., Yamazaki, K., Noda, T., Yamori, T. and Shiba, K. (2004). Synthesis of functional proteins by mixing peptide motifs. *Chem. Biol.* **11**, 765-773.
Saito, H., Kashida, S., Inoue, T. and Shiba, K. (2007). The role of peptide motifs in the evolution of a protein network. *Nucleic Acids Res.* **35**, 6357-6366.
Santos-Sacchi, J. (1991). Reversible inhibition of voltage-dependent outer hair cell motility and capacitance. *J. Neurosci.* **11**, 3096-3110.
Santos-Sacchi, J., Shen, W., Zheng, J., Dallos, P. (2001). Effects of membrane potential and tension on prestin, the outer hair cell lateral membrane motor protein. *J. Physiol.* **531**, 661-666.
Schaechinger, T. J. and Oliver, D. (2007). Nonmammalian orthologs of prestin (SLC26A5) are electrogenic divalent/chloride anion exchangers. *Proc. Natl. Acad. Sci. USA* **104**, 7693-7698.
Schaechinger, T. J., Gorbunov, D., Halaszovich, C. R., Moser, T., Kügler, S., Fakler, B. and Oliver, D. (2011). A synthetic prestin reveals protein domains and molecular operation of outer hair cell piezoelectricity. *EMBO J*. **30**, 2793-2804.
Seymour, M. L., Rajagopalan, L., Volk, M. J., Liu, H., Brownell, W. E. and Pereira, F. A. (2011). Membrane prestin expression correlates with magnitude of prestin-associated charge movement. *Assoc. Res. Otolaryngol. Abs*. **34**, 22.
Tan, X., Pecka, J. L., Tang, J., Okoruwa, O. E., Zhang, Q., Beisel, K. W. and He, D. Z. (2011). From zebrafish to mammal: functional evolution of prestin, the motor protein of cochlear outer hair cells. *J. Neurophysiol.* **105**, 36-44.
Tang, J., Pecka, J. L., Tan, X., Beisel, K. W. and He, D. Z. Z. (2011). Engineered pendrin protein, an anion transporter and molecular motor. *J. Biol. Chem.* **86**, 31014-31021.
Zhang, P. C., Keleshian, A. M. and Sachs, F. (2001). Voltage-induced membrane movement. *Nature* **413**, 428-432.
Zheng, J., Shen, W., He, D. Z., Long, K. B., Madison, L. D. and Dallos, P. (2000). Prestin is the motor protein of cochlear outer hair cells. *Nature* **405**, 149-155.